A&A 488, 685–696 (2008)
DOI: 10.1051/0004-6361:200809867

Astronomy & Astrophysics

Testing the forward modeling approach in asteroseismology

I. Seismic solutions for the hot B subdwarf Balloon 090100001 with and without a priori mode identification⋆

V. Van Grootel[1,2], S. Charpinet[1], G. Fontaine[2], P. Brassard[2], E. M. Green[3], P. Chayer[4], and S. K. Randall[5]

[1] Laboratoire d'Astrophysique de Toulouse-Tarbes, Université de Toulouse, CNRS, 14 av. E. Belin, 31400 Toulouse, France
e-mail: [valerie.vangrootel;stephane,charpinet]@ast.obs-mip.fr
[2] Département de Physique, Université de Montréal, CP 6128, Succursale Centre-Ville, Montréal, QC H3C 3J7, Canada
e-mail: [fontaine;brassard]@astro.umontreal.ca
[3] Steward Observatory, University of Arizona, 933 North Cherry Av., Tucson, AZ 85721, USA
e-mail: bgreen@as.arizona.edu
[4] Space Telescope Science Institute, 3700 San Martin Drive, Baltimore, MD 21218, USA
e-mail: chayer@stsci.edu
[5] ESO, Karl-Schwarzschild-Str. 2, 85748 Garching bei München, Germany
e-mail: srandall@eso.org

Received 28 March 2008 / Accepted 1 July 2008

ABSTRACT

Context. Balloon 090100001, the brightest of the known pulsating hot B subdwarfs, exhibits simultaneoulsy both short- and long-period pulsation modes, and shows relatively large amplitudes for its dominant modes. For these reasons, it has been studied extensively over the past few years, including a successful experiment carried out at the Canada-France-Hawaii Telescope to pin down or constrain the value of the degree index ℓ of several pulsation modes through multicolor photometry.
Aims. The primary goal of this paper is to take advantage of such partial mode identification to test the robustness of our standard approach to the asteroseismology of pulsating subdwarf B stars. The latter is based on the forward approach whereby a model that best matches the observed periods is searched for in parameter space with no a priori assumption about mode identification. When successful, this method leads to the determination of the global structural parameters of the pulsator. As a bonus, it also leads, after the fact, to complete mode identification. For the first time, with the availability of partial mode identification for Balloon 090100001, we are able to evaluate the sensitivity of the inferred seismic model to possible uncertainty in mode identification.
Methods. We carry out a number of exercises based on the double optimization technique that we developed within the framework of the forward modeling approach in asteroseismology. We use the set of ten periods corresponding to the independent pulsation modes for which values of ℓ have been either formally identified or constrained through multicolor photometry in Balloon 090100001. These exercises differ in that they assume different a priori mode identification.
Results. Our primary result is that the asteroseismic solution stands very robust, whether or not external constraints on the values of the degree ℓ are used. Although this may come as a small surprise, the test proves to be conclusive, and small differences in mode identification among the ten modes do not affect in any significant way, at the typical accuracy presently achieved, the final emergent seismic model. This is due to the structure of the p-mode pulsation spectra in sdB stars. In all cases, the inferred structural parameters of Balloon 090100001 remain practically unchanged. They correspond, and this constitutes our second important result, to a star beyond the TAEHB with $T_{\rm eff} = 28\,000 \pm 1\,200$ K, $\log g = 5.383 \pm 0.004$, $M_*/M_\odot = 0.432 \pm 0.015$, and $\log M_{\rm env}/M_* = -4.89 \pm 0.14$. Other structural parameters are also derived.

Key words. stars: oscillations – stars: interiors – stars: subdwarfs – stars: individual: Balloon 090100001

1. Introduction

The hot subdwarf B (sdB) stars are core-helium burning objects with masses around 0.5 $M_\odot$ surrounded by very thin hydrogen-rich envelopes ($M_{\rm env} < 0.02\ M_\odot$). With effective temperatures between 20 000 and 40 000 K and surface gravities $\log g$ in the range 5.0–6.2, they are identified with models of the extreme horizontal branch (EHB) stars (Heber 1986). Subdwarf B stars are found in our Galaxy both in the old disk (field stars) and as globular cluster members (halo population). They dominate the populations of faint blue objects down to $V \sim 16$, and are most likely the main source of the UV excess (the so-called UV-upturn phenomenon) observed in elliptical galaxies (Brown et al. 1997).

Interest in this particular phase of stellar evolution has increased spectacularly in recent years with the discoveries of two distinct classes of pulsators among sdB stars. This has opened up the opportunity of using the power of asteroseismology to study them. This development is most welcome because understanding the details of the formation process of sdB stars has remained quite a challenge (see, e.g., Dorman et al. 1993; D'Cruz et al. 1996; Han et al. 2002, 2003). It is hoped that asteroseismology will help discriminate between the various competing scenarios

⋆ Based on photometric observations obtained at the Canada-France-Hawaii Telescope (CFHT) which is operated by the National Research Council of Canada, the Institut National des Sciences de l'Univers of the Centre National de la Recherche Scientifique of France, and the University of Hawaii. Some of the spectroscopic observations reported here were obtained at the MMT Observatory, a joint facility of the University of Arizona and the Smithsonian Institution.

that have been proposed to account for the very existence of the sdB stars. Among others, asteroseismology should be especially useful for establishing the mass distribution of sdB stars, the latter bearing the signature of the formation channel, and it is one of the long-range goals that we are aiming at.

The rapid sdB pulsators, commonly referred to as EC 14026 stars or, more officially, V361 Hya stars, were the first to have been observationally detected (Kilkenny et al. 1997). Their existence was independently predicted through pure theoretical considerations (Charpinet et al. 1996, 1997). The pulsations in EC 14026 stars are characterized by multiperiodic, low-amplitude, and short-period (80−600 s) luminosity variations. The presence of excited pulsation modes, usually low-degree, low-order acoustic modes, is well understood through the action of a classic κ-mechanism powered by local accumulations of iron due to radiative levitation (Charpinet et al. 2001). Beyond iron, the importance of nickel on the opacity profile, as well as the opacity sources themselves, have been underlined by Jeffery & Saio (2006, 2007).

More recently, a second family of pulsating sdB stars, named PG 1716 stars after the prototype (now officially the V1093 Her stars), was observationally discovered by Green et al. (2003). Those are again multiperiodic and low-amplitude pulsators, but with much longer periods, in the range 2000−9000 s. This immediately implies the presence of mid-order, low-degree g-modes. Such g-modes have been shown to be also driven by the same mechanism responsible for the pulsations in EC 14026 stars (Fontaine et al. 2003). Quite interestingly, two objects identified initially as short-period pulsators have also been found recently to exhibit long-period oscillations as well: HS 0702+6043 (Schuh et al. 2006) and Balloon 090100001 (Oreiro et al. 2005). Even more recently, a new member of this hybrid class, HS 2201+2610, was announced during the Third Meeting on Hot Subdwarf Stars and Related Objects held in Bamberg in 2007 July (Lutz et al. 2008).

In the surface gravity-effective temperature plane, the short-period pulsators tend to cluster at high effective temperatures and high surface gravities, while long-period pulsators populate the low-temperature, low-gravity part of the domain where sdB stars are found. While the long-period pulsators have proven more difficult so far to interpret quantitatively (see, e.g., Randall et al. 2006a), the group of short-period pulsators has already provided excellent opportunities for the asteroseismic determination of the basic structural parameters of sdB stars. To date, asteroseismological analyses of this sort have been carried out for seven EC 14026 pulsators: PG 0014+067 (Brassard et al. 2001), PG 1047+003 (Charpinet et al. 2003), PG 1219+534 (Charpinet et al. 2005a), Feige 48 (Charpinet et al. 2005b; Van Grootel et al. 2008), EC 20117−4014 (Randall et al. 2006b), PG 1325+101 (Charpinet et al. 2006), and PG 0911+456 (Randall et al. 2007). In all cases, no a priori mode identification was available, so the derived seismic models have remained largely untested from that particular point of view. However, we emphasize that these models are able to reproduce simultaneously all the observed periods at a satisfactory level of accuracy, while being entirely consistent with the predictions of nonadiabatic theory and, at the same time, satisfying independent constraints imposed by time-averaged spectroscopy. Moreover, total and envelope masses derived from these models are found in the range expected for core helium burning stars from stellar evolution. Still, it remains highly desirable to verify by independent means the derived mode identification if at all possible.

In this context, the hybrid pulsator Balloon 090100001 (hereafter BAL 0901) has stood out as an obvious candidate for partial mode identification through multicolor photometry or time-resolved spectroscopy because of its brightness ($V = 12.1$), the richness of its pulsation spectrum, and the unusually large amplitudes of its dominant modes (see, e.g., Baran et al. 2006). For these reasons, BAL 0901 has been observed and studied extensively over the recent past, including, for example, *UBVR* photometry reported by Baran et al. (2005) and analyzed by Tremblay et al. (2006), and time-resolved spectroscopy carried out at the Nordic Optical Telescope in August/September 2004 (Telting & Østensen 2006). Notably, Baran et al. (2008) recently reused these two sets of observations that were coincidentally obtained at the same time and proposed ℓ-identifications for the five dominant modes based on a combined analysis of the multicolor photometry and the spectroscopy. Also recently, Pereira et al. (2008) reported on the results of a high-sensitivity multisite campaign which has uncovered well over 50 distinct oscillation modes in the white light pulsation spectrum of BAL 0901. As part of that campaign, *UBV* photometry was gathered at the Canada-France-Hawaii Telescope. The quality of these observations was sufficient to allow the formal identification (or to constrain) the ℓ index of ten different modes in BAL 0901, excluding fine-structure frequency multiplets presumably due to slow rotation. This was done following the procedure explained in Randall et al. (2005; and see also Tremblay et al. 2006). Preliminary results of this multicolor analysis have been presented in Charpinet et al. (2008), and a full report will be provided in Brassard et al. (2008, in preparation).

In the present work, we take advantage of the availability of the partial ℓ identification already obtained in BAL 0901 to investigate the sensitivity of the inferred seismic model to a priori mode identifications and/or constraints. Specifically, we carry out asteroseismological exercises in the forward method by best-fitting the set of ten periods for which we have constraints on their degree indices ℓ. This number of independent modes is typical of the available number of periods used in our previous studies of other EC 14026 pulsators. Note that all the ten retained pulsation modes belong to the short-period branch of the pulsation spectrum of this hybrid pulsator. No useful constraints have been derived yet from multicolor photometry for the long-period modes because they show relatively small amplitudes, although this may change with more refined analyses.

We discuss the available estimates of the atmospheric parameters of BAL 0901 in Sect. 2, and we present our own values based on new time-averaged spectra gathered at Steward Observatory. This is done to verify that the retained seismic models remain consistent with the independent constraints imposed by spectroscopy on the atmospheric parameters of the star. We next present, in Sect. 3, the results of our asteroseismic analyses using the ten periods alluded to above. We consider the cases in which "weak" constraints and "strong" constraints on the ℓ values are imposed at the beginning of the search exercises in parameter space. We also discuss the test case in which no a priori ℓ identifications are used, except for general considerations based on standard visibility arguments. We finally provide a discussion and summary of our main results in the last section.

2. Atmospheric parameters from spectroscopy

BAL 0901 got its designation as an object identified in a survey carried out with a 13 cm balloon-borne telescope designed to detect FUV-bright objects (Bixler et al. 1991). These authors derived the first estimates of its atmospheric parameters, $T_{\rm eff} = 32\,500 \pm 6700$ K, $\log g = 6.00 \pm 0.69$, and $\log N({\rm He})/N({\rm H}) < -2.00$, leaving no doubt as to the sdB

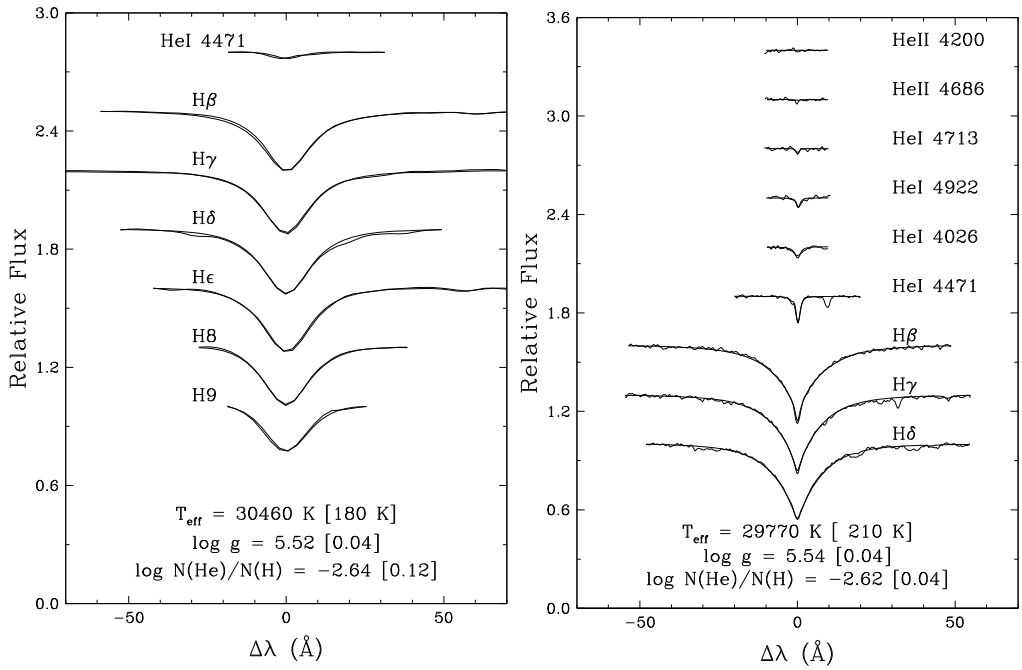

Fig. 1. *Left panel*: model fit (heavy curve) to the hydrogen Balmer lines and helium lines (thin curve) available in our time-averaged, high S/N ratio, low-resolution optical spectrum of BAL 0901 obtained at the Steward 2.3 m telescope on Kitt Peak. *Right panel*: model fit (heavy curve) to the hydrogen Balmer lines and helium lines (thin curve) available in our time-averaged, high S/N ratio, mid-resolution MMT optical spectrum of BAL 0901. Note the presence of several weak metal lines that have become visible at this better resolution, notably the Fe III 4372 line in the red wing of Hγ and the Mg II 4481 line next to the He I 4471 feature.

nature of the object. Much improved estimates of these parameters were obtained later by Oreiro et al. (2004) in their important paper reporting, for the first time, the presence of short-period oscillations in that star. These authors used a grid of metal-blanketed LTE model atmospheres and synthetic spectra made available to them by U. Heber (see, e.g., Heber et al. 2000) to analyze an intermediate-resolution spectrum of BAL 0901 obtained at the William Herschel Telescope. While no metal lines were visible at that resolution, the models assumed the presence of metals in solar proportions. The derived parameters are $T_{\rm eff}$ = 29 446 ± 500 K, log g = 5.33 ± 0.10, and log N(He)/N(H) = −2.54 ± 0.20. Using the same grid of LTE models with solar metallicity, Østensen, Telting & Heber (2007) analyzed a series of time-resolved low-resolution spectra obtained subsequently at the Nordic Optical Telescope. In their interesting experiment, they were able to estimate the apparent variations in log g and $T_{\rm eff}$ during the pulsation cycles of BAL 0901. Their mean spectrum showed a superb S/N ratio, and the derived values of the time-averaged atmospheric parameters turned out to be fully consistent with those of Oreiro et al. (2004), i.e., $T_{\rm eff}$ = 28 883 ± 1186 K, log g = 5.416 ± 0.084, and log N(He)/N(H) = −2.730 ± 0.003[1]. These values from two independent data sets are also consistent with the earlier estimates of Bixler et al. (1991), but are far more accurate. They place BAL 0901 on the cool side of the EC 14026 instability region in the log g − $T_{\rm eff}$ plane, in fact at the common boundary with the PG1716 stars domain, quite a fitting place for a hybrid pulsator.

We also obtained additional spectra of BAL 0901 with the 6.5 m Multiple Mirror Telescope (MMT) and the Steward Observatory 2.3 m telescope on Kitt Peak, Arizona, as part of our global program aimed at the homogeneous determinations of surface parameters for sdB stars (Green et al., in preparation). The MMT spectrum covers the ∼4000−5000 Å region with a medium wavelength resolution of ∼1 Å, while the Kitt Peak data cover the ∼3600−5500 Å range at a lower resolution of ∼9 Å. The latter spectrum is characterized by an exquisite value of S/N ∼ 490, whereas the former shows a more modest, but still excellent S/N ratio of about 200. A simultaneous fit of the available Balmer lines (Hβ to Hδ for the medium-resolution spectrum and Hβ to H9 for the low-resolution spectrum) and helium lines using synthetic spectra culled from a grid of NLTE H/He model atmospheres was performed for each available spectrum. We show in Fig. 1 the best model fit for the 2.3 m (left panel) and the MMT (right panel) spectrum, where the quoted uncertainties on the parameters correspond only to the formal errors of the fit. By adding quadratically to these errors the external uncertainties estimated from multiple observations of the same stars, we obtain $T_{\rm eff}$ = 30 460 ± 300 K, log g = 5.52 ± 0.06, and log N(He)/N(H) = −2.64 ± 0.12 from the 2.3 m spectrum, and $T_{\rm eff}$ = 29 770 ± 425 K, log g = 5.54 ± 0.06, and log N(He)/N(H) = −2.62 ± 0.04 from the MMT spectrum.

Although these two sets of estimates for the atmospheric parameters of BAL 0901 are impressively consistent with each other, there appears to be a slight systematic deviation with respect to the results of Oreiro et al. (2004) and those of Østensen et al. (2007) in the sense that our values for log g and $T_{\rm eff}$ come out a little larger than those of these authors. Since we fix the effective temperature of the seismic model at the outset from spectroscopy ($T_{\rm eff}$ cannot be determined more accurately from asteroseismology because p-mode periods in sdB stars depend only weakly on it), it seems important to understand these systematic trends between various authors, at least qualitatively. At first sight, this argument comes out much less strongly for the surface gravity because, as is now well known, and contrary to the effective temperature, the pulsation periods are very sensitive

[1] The quoted uncertainties, which appear relatively large for $T_{\rm eff}$ and log g, may not do full justice to the results of Østensen et al. (2007), but we could not find more appropriate values in their paper.

to a variation in log g, and asteroseismology does provide much more accurate estimates of that parameter than spectroscopy can. Still, it is generally quite useful to have the best possible independent spectroscopic constraints on the value of log g in order to discriminate, as needed, between various possible seismic solutions having different inferred surface gravities.

We recall here that Oreiro et al. (2004) and Østensen et al. (2007) have analyzed their spectra with a set of LTE model atmospheres with solar metallicity, whereas we used full NLTE H/He models, but with no metals. A close examination of our MMT spectrum readily reveals several weak metal lines (see Fig. 1, right panel). In the absence of a detailed abundance analysis, which would be way beyond the scope of this paper, we still attempted to estimate some ion abundances using the measured equivalent widths of features such as C II 4267, N II 4237-4241, O II 4649, Mg II 4481, Si III 4568-4575, S III 4253, and Fe III 4164-4372. Our crude analysis revealed that BAL 0901 is not necessarily exceptional in terms of metal abundances compared to other sdB stars, but it does contain heavy elements. In particular, we find that its atmospheric abundance of iron comes out slightly larger than solar, log N(Fe)/N(H) $= -4.27$ (with some large uncertainty), which is rather the norm for these objects (see, e.g., Edelmann 2003 or Blanchette et al. 2008). In view of this, we conclude that our estimates $T_{\rm eff} \simeq 30\,100$ K and log $g \simeq 5.53$ are probably a little skewed by our ignorance of metals in our NLTE model calculations.

To explore that question further, we computed some more models in full NLTE but, this time, we included C, N, O, and Fe in solar proportions along with H and He. It should be pointed out that the role of iron in this is fundamental because it provides most of the extra opacity in the atmospheric layers. This is really the key element in this experiment. It should also be realized that adding only a few extra elements – as we did – slows down considerably the computations of NLTE models, and this largely explains why we do not have a full grid of these, especially in the spirit of this exploratory work. We find that adding metals in the models decreases both our estimates of log g and $T_{\rm eff}$ for BAL 0901. For instance, a NLTE model spectrum with metals and specified by log $g = 5.35$, $T_{\rm eff} = 28\,000$ K, and log N(He)/N(H) $= -2.60$ is interpreted through our grid of NLTE H/He models with no metals (following our standard procedure for the observed spectra above) as a star with log $g = 5.54$, $T_{\rm eff} = 30\,096$ K, and log N(He)/N(H) $= -2.62$. Those values fall almost exactly on our derived parameters for BAL 0901. In the absence of a detailed self-consistent abundance analysis for BAL 0901, we therefore adopt "corrections" of $\Delta T_{\rm eff} = -2096$ K, Δlog $g = -0.19$ dex, and Δlog N(He)/N(H) $= +0.02$ dex to be applied to our previous values discussed above. We believe that these revised estimates reflect better the physical state in the atmosphere of BAL 0901 which, in fact, does contain metals. In particular, we suggest that the true effective temperature of BAL 0901 is closer to 28 000 K than 30 100 K found above, and this is the value that we adopt below in our asteroseismological exercises. To reflect the fact that detailed metal abundances are currently lacking, we allow for a generous uncertainty and adopt $T_{\rm eff} = 28\,000 \pm 1200$ K as our best estimate of the effective temperature of BAL 0901.

3. Asteroseismic analysis

3.1. Numerical tools for asteroseismic analysis

The procedure developed to perform objective asteroseismic analyses of sdB pulsators has been described at length in Charpinet et al. (2005a). This method is a forward modeling approach based on the specific requirement of *global* optimization, i.e., pulsation spectra computed from sdB models must match *all* the observed periods *simultaneously*. The first step consists in calculating the internal structure of the subdwarf star from four fundamental parameters: the effective temperature $T_{\rm eff}$, the surface gravity log g, the total mass of the star M_*, and the logarithmic fractional mass of the hydrogen-rich envelope log q(H) evaluated at the halfway point in the thin H-envelope/He-mantle transition layer[2]. These so-called "second generation" models of subdwarf B stars are static structures made of an inert hard ball nucleus surrounded by a detailed mantle/envelope extending as deep as log $q \equiv \log(1-M(r)/M_*) \simeq -0.05$. They incorporate the variable nonuniform abundance profile of iron predicted by microscopic diffusion assuming an equilibrium between gravitational settling and radiative levitation. They are particularly well suited for modeling p-modes in pulsating sdB stars. In a second step, pulsations properties of the models are evaluated through the consecutive application of improved versions of the linear adiabatic and nonadiabatic pulsation codes described briefly in Brassard et al. (1992) and Fontaine & Brassard (1994), respectively. For each pulsation mode analyzed, these codes provide the period $P_{\rm th}$ ($= 2\pi/\sigma_{\rm R}$, where $\sigma_{\rm R}$ is the real part of the complex eigenfrequency) and the stability coefficient σ_I (the imaginary part of the eigenfrequency). If σ_I is positive, the mode is stable (damped), while the contrary holds if σ_I is negative: the mode is then excited and may therefore reach an observable amplitude. In an ideal situation, all the pulsation modes detected in a real star should then be associated with unstable theoretical modes. Other quantities that come out of the nonadiabatic code for each pulsation mode are the kinetic energy E (particularly interesting for theoretical studies such as, e.g., mode trapping), and the dimensionless first-order solid rotation coefficient C_{kl}. As is standard, the pulsation calculations are performed assuming perfect spherical symmetry (each mode is $2\ell + 1$ fold-degenerate in eigenfrequency), which is fully justified for slow rotating stars such as BAL 0901. Hence, all multiplet components seen in the pulsation spectrum have to be considered as a single independent mode for the asteroseismic analysis, and the fine structure is interpreted *a posteriori* in terms of slow rotation that lifts the $2\ell + 1$ fold-degeneracy of the mode periods (see Sect. 3.4). In this context, a pulsation mode is then completely defined in terms of its radial order k and its degree index ℓ. The spectrum of computed periods is then employed in a double optimization procedure to isolate and quantify the best-fitting models that minimize the merit function,

$$S^2 = \sum_{i=1}^{N_{\rm obs}} \left(\frac{P^i_{\rm obs} - P^i_{\rm th}}{\sigma_i} \right)^2 , \qquad (1)$$

where $N_{\rm obs}$ is the number of independent observed periodicities used in the asteroseismic analysis, ten in the present case, and σ_i is a weight that can be associated to each pair of periods. Following previous studies (see, e.g., Brassard et al. 2001), we usually adopt here a global weight which is the inverse of the theoretical mode density of each model, i.e., we set $\sigma_i = \sigma_d$, where σ_d is the ratio of the width of the considered period window (here 700 s; see Sect. 3.2) to the number of modes in that window. This technical choice has no incidence on the position

[2] This parameter is intimately related to the more familiar parameter $M_{\rm env}$, the total mass of the hydrogen-rich envelope, that includes the small extra mass of hydrogen contained in the lower half of the thin H/He transition zone, through the relation log[$M_{\rm env}/M_*$] = log q(H) + C, where C is a small positive model-dependent term.

Table 1. Derived identification of the geometrical degree index ℓ for ten groups of modes observed in BAL 0901, including the rotationally-split components. The underlined period within a multiplet group is that considered as the central $m = 0$ component used for the asteroseismic analysis. This reproduces the results of the multicolor analysis presented by Charpinet et al. (2008) as given in their Table 1.

Period (s)	Strong ℓ constraints	Weak ℓ constraints
356.194	0	0
354.205, 354.008, 353.809	1	1
350.392, 350.171, 349.831	2	2
264.892	0	0, 1
263.819, 263.736	4	4
261.444, 261.216	1	1, 2
253.514	2	1, 2
215.454, 215.291	1	0, 1
214.610, 214.374	2	1, 2
201.430	1	0, 1, 2

of the solutions and, therefore, on the final results. It simply removes, at least partially, possible large scale biases toward unrealistic models (usually found at the low $\log g$ boundary of the explored parameter space) having higher mode densities than the observed spectrum. This is principally meant to prevent the minimization code (see below) from allocating too much ressources (at the cost of a reduced computational efficiency) in regions with denser period spectra (at low $\log g$) in clear conflict with spectroscopy, anyway. For a given model, and using or not external constraints on the ℓ values as may be appropriate, a first optimization step leads to the mode identification (k, ℓ) corresponding to the best possible simultaneous match of all the ten observed periods with ten periods belonging to the theoretical spectrum of that model. Finally, the second optimization phase is aimed at uncovering the best period-matching models in parameter space by finding minima of the function $S^2(T_{\rm eff}, \log g, \log q(\mathrm{H}), M_*)$ with a dedicated optimization code based on a hybrid Genetic Algorithm (GA) designed to explore the vast model parameter space. These optimal models therefore constitute the asteroseismological solutions.

In the case of BAL 0901, we took advantage of the availability of the partial mode identification (i.e., the degree index ℓ) obtained previously through multicolor photometry. Charpinet et al. (2008) presented a preliminary analysis of an outstanding *UBV* data set on BAL 0901 obtained at the Canada-France-Hawaii Telescope, which led to the formal identifications or to useful constraints on the values of ℓ for ten different pulsation modes. Note that the light curve of BAL 0901 contains many more pulsations (see, e.g., Baran et al. 2005, 2006 or Pereira et al. 2008), but only the ten modes retained by Charpinet et al. (2008) – excluding their multiplet components – have amplitudes large enough for useful mode identification to have been achieved through the amplitude ratios method based on multicolor photometry. In order to be able to carry out the test described in the Introduction, we therefore limited ourselves to these ten modes in our asteroseismological investigations.

The results of Charpinet et al. (2008) are summarized in Table 1. Among the ten groups of modes identified, six show a multiplet structure best interpreted as due to rotational splitting. In those cases, only the $m = 0$ component (the number underlined in each multiplet) has been used in our analysis. Following Randall et al. (2005), a formal identification procedure based on a Q-probability formalism has been applied in the χ^2 method followed by Charpinet et al. (2008) to identify the ℓ value of each of the retained pulsation modes in BAL 0901. The χ^2 approach minimizes the differences between the three observed amplitudes and the predicted ones in the U, B, and V bandpasses for each mode. A formal identification for the degree index was then achieved if only one of the six values considered ($\ell = 0$–5) led to a value of χ^2 lower than a statistically significant level as computed by the Q-probability method. This was achieved for four modes as indicated in Table 1 (third column). In the other six cases, no unique solutions were found, but still quite useful constraints were also derived as two (or three in one instance) values of ℓ led to χ^2 values that were formally acceptable for a given mode. The third column in Table 1 shows the final results of Charpinet et al. (2008). We use these constraints below to carry out a first asteroseismological analysis, which we consider as our reference one. As a measure of comparison, we also retained the best ℓ solution (that providing the smallest value of χ^2) in those cases where two (or three) values are formally acceptable. This led to the identification summarized in the second column of Table 1. In what follows, we refer to this set of ℓ values as that providing "strong" constraints since all ten modes are identified a priori. The set listed in the third column of the table provides, in comparison, only "weak" constraints (but it is the one that remains formally acceptable).

3.2. Search for the optimal model

In the first application of the optimization procedure, the weak constraints are assumed, i.e., the asteroseismic analysis is carried out by constraining the values of the ℓ degree to all formally acceptable values from multicolor photometry. In the second experiment, we redo the analysis by imposing the preferred values of ℓ for each period (the strong constraints). Finally, in the third application of the entire procedure, no a priori constraints on the mode identification are used, except for the general assumption that all ten modes must belong to either degree $\ell = 0$, 1, 2, or 4. We explicitly exclude the possibility that the modes with degree indices $\ell = 3$ and $\ell \geq 5$ would be present because they are expected to be less visible in the optical domain (see Randall et al. 2005). The comparison between the results obtained under the three assumptions constitutes therefore a crucial test of our general approach to the asteroseismology of sdB stars, at the level of the mode identification of course, but much more importantly in our view, at the level of the reliability and robustness of the stellar model parameters inferred from each optimal solution.

In all three exercises, the asteroseismic analysis is performed in a three-dimensional parameter space defined by the surface gravity $\log g$, the envelope thickness $\log q(\mathrm{H})$, and the stellar mass M_*. The effective temperature is set to the value found from spectroscopy (i.e., $T_{\rm eff} = 28\,000$ K) as this approach leads to the best possible estimate as discussed briefly above. The initial boundaries for the search parameter domain were set as follows: $5.3 \leq \log g \leq 5.6$, $-5.2 \leq \log q(\mathrm{H}) \leq -2.0$, $0.3 \leq M_*/M_\odot \leq 0.7$. The limits on the surface gravity cover a generous range about the values suggested by spectroscopy, keeping in mind the problem of metals that also affects this parameter. The constraints on $\log q(\mathrm{H})$ and M_* rely on stellar evolution theory and various formation scenarios (Han et al. 2002, 2003). We also mention that the theoretical periods were computed in the range 100–800 s (covering amply the observed range for the periods of BAL 0901).

Within the search domain just specified, the optimization procedure in our first experiment – that relying on the weak

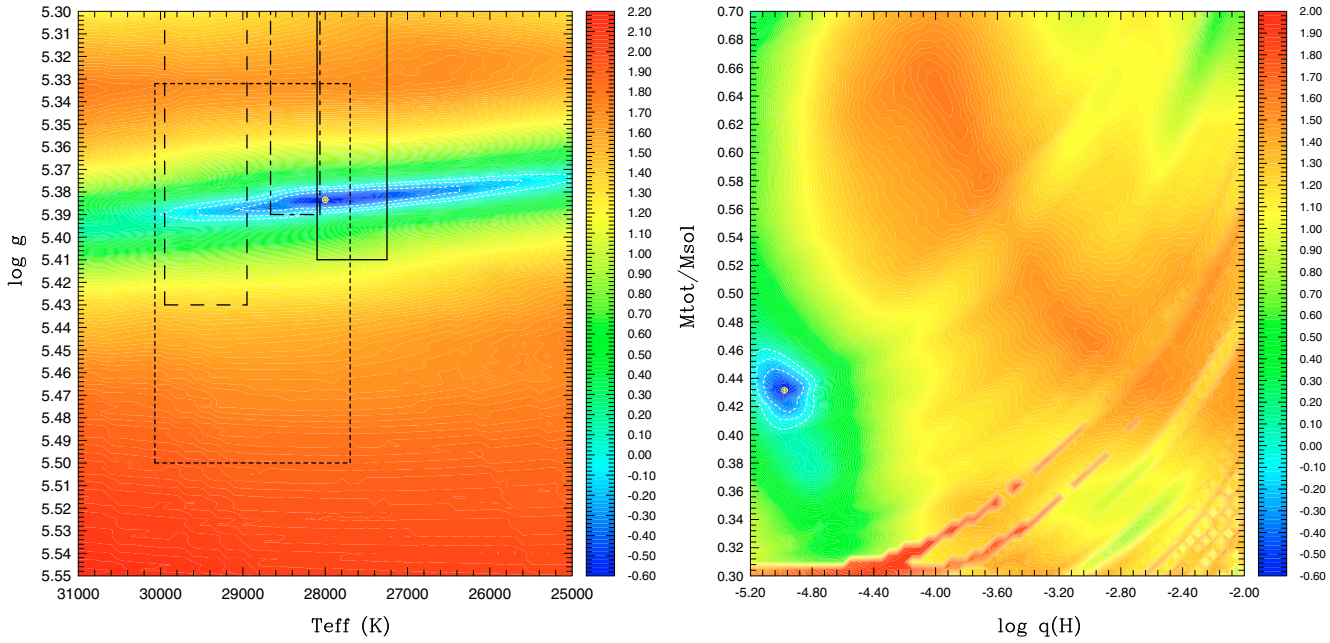

Fig. 2. *Left panel:* slice of the S^2 function (in logarithmic units) along the $\log g - T_{\rm eff}$ plane at fixed parameters M_* and $\log q$(H) set to their optimal values as obtained in our reference study, that using the weak constraints on the ℓ values of the ten pulsation modes. The solid and dot-dashed rectangles show, respectively, the spectroscopic inferences made from our MMT and 2.3 m telescope spectra. The dashed rectangle illustrates the spectroscopic solution given by Oreiro et al. (2004), while the dotted rectangle shows that provided by Østensen et al. (2007). *Right panel:* slice of the S^2 function (in logarithmic units) along the $M_*-\log q$(H) plane at fixed parameters $\log g$ and $T_{\rm eff}$ set to their optimal values as obtained in our reference study. In both panels, the best-fit model is indicated by a yellow mark, and white dashed contours are the 1, 2, and 3σ limits.

constraints on ℓ – led to the identification of one clear and very well defined optimal solution, and no significant secondary minima were found. At fixed $T_{\rm eff} = 28\,000$ K, this best-fit solution shows a merit function of $S^2 \simeq 0.249$, and corresponds to a model with $\log g = 5.383$, $\log q$(H) $= -4.98$, and $M_* = 0.432\ M_\odot$. Figure 2 illustrates the behavior of the S^2 hypersurface in the vicinity of the solution (indicated by a yellow mark). This figure shows slices of the merit function along the $\log g - T_{\rm eff}$ plane (at fixed parameters M_* and $\log q$(H) set to their optimal values) in the left panel, and along the $M_* - \log q$(H) plane (at fixed parameters $T_{\rm eff}$ and $\log g$ set to their optimal values) in the right panel. The blue areas, corresponding to low values of S^2, harbor the best-fitting models, while the red areas represent comparatively bad fits, i.e., where theoretical periods computed from models do not fit well the observed periods. Considering the logarithmic scale used to represent the merit function in these figures, the blue regions correspond indeed to very well defined minima. The significance of these minima can be evaluated more quantitatively by linking the merit function, S^2, to the standard reduced χ^2 formalism. This was first introduced and discussed in some detail in Sect. 3.5 of Brassard et al. (2001) in order to estimate the uncertainties associated with the derived model parameters. We refer the reader to this work for a complete description of the procedure. We stress, in particular, that the quantity $\Delta\chi^2_{\rm std}$ that is added to the minimum value of a standard χ^2 to define the 1σ confidence level must be renormalized to the scale of the S^2-values. In the present case, this leads to $\Delta S^2_{1\sigma} \simeq 0.291$ which, when added to the S^2-value of the optimal solution, provides the 1σ confidence level shown in Fig. 2 (the 2σ and 3σ limits are also given in that figure). This quantity, $\Delta S^2_{1\sigma}$, is also used to estimate the errors on the derived stellar parameters of BAL 0901 (see Sect. 3.4).

The boxes in the left hand panel of Fig. 2 indicate the four spectroscopic measurements available, two of which, in our case, have been shifted by the metal "correction vector" described above. While we did use available spectroscopy to fix the effective temperature and define a search interval in surface gravity that would be consistent with it at the outset, we wish to point out that there is never any a priori guarantee in this kind of exercise that an asteroseismological solution will be found within the search domain. The fact that, once again for this 8th EC 14026 pulsator (see the Introduction), we found one such solution consistent with the available spectroscopic measurements demonstrates that our approach to the asteroseismology of sdB stars must be sound. We also wish to point out that the horizontal band in red in the left hand side panel of Fig. 2 corresponding to values of $\log g \simeq 5.52-5.54$ as estimated in our initial analysis using NLTE models *with no metals* indicate very bad fits to the pulsation data. Simply put, the ten observed periods in BAL 0901 rule out a value of the surface gravity as large as those for that star.

It is extremely interesting and instructive to compare the results of this first asteroseismological exercise with those of two other experiments. In the second one, as explained above, we used strong constraints and fixed the value of ℓ for each of the ten modes according to its preferred estimate from multicolor photometry. This led to an optimal merit function of $S^2 \simeq 0.290$ (only marginally degraded compared to the previous one, as the difference is below 1σ), corresponding to a nearly identical seismic model with $\log g = 5.382$, $\log q$(H) $= -5.01$ and $M_* = 0.430\ M_\odot$. In this, the effective temperature is still fixed to 28 000 K via spectroscopic arguments. In the third experiment, we did not impose a priori constraints on the values of ℓ, except for general restrictions related to visibility arguments as discussed above. This situation is representative of what has been done before in the past for other pulsators. As expected, with less constraints, the merit function could only improve, here to a slightly – but not significantly – better value of $S^2 \simeq 0.166$, i.e.,

Table 2. Mode identification obtained for each optimal model derived by imposing strong, weak, and no a priori constraints on the values of ℓ. In all cases, the effective temperature is fixed to 28 000 K.

		Strong		Weak		No	
Frequency	Period	constraints		constraints		constraints	
(μHz)	(s)	ℓ	k	ℓ	k	ℓ	k
2807.46	356.194	0	0	0	0	**2**	0
2824.79	354.008	1	1	1	1	**0**	**0**
2855.75	350.171	2	1	2	1	**4**	**0**
3775.12	264.892	0	2	0	2	0	2
3791.67	263.736	4	2	4	2	4	2
3824.91	261.444	1	3	1	3	1	3
3944.55	253.514	2	3	2	3	2	3
4644.88	215.291	1	4	1	4	1	4
4664.74	214.374	2	4	2	4	2	4
4964.50	201.430	1	5	**0**	**4**	**4**	**4**
S^2		0.290		0.249		0.166	
log g		5.382		5.383		5.385	
$M_*/M_\odot$		0.430		0.432		0.432	
$\log(M_{\rm env}/M_*)$		−4.92		−4.89		−4.86	

still within $\Delta S^2_{1\sigma}$ of the solution obtained with the weak constraints. Most remarkably, however, the solution led to a seismic model with log g = 5.385, log q(H) = −4.96 and M_* = 0.432 $M_\odot$, virtually the same as that inferred in our first experiment! There cannot be more convincing demonstration of the robustness of the inferred seismic solution against uncertainties in mode identification.

Table 2 lists the frequencies and periods of the ten observed modes of interest in BAL 0901 (first two columns), along with the complete mode identifications (i.e., in terms of the degree index ℓ *and* of the radial order k) inferred in each of our three numerical experiments. The primary structural parameters of the optimal model derived in these experiments are also listed in the lower half of the table. By construction, the values of ℓ have been fixed in advance in our exercise involving strong constraints. Only the k values were thus derived from the optimization procedure, and those are reported in the first group of two columns pertaining to mode identification. In comparison, by imposing looser constraints on ℓ obtained from the formal solution of the multicolor analysis (see Table 1, third column), we obtained the results given in the second group of two columns. It is interesting to point out that the optimization procedure in this case led naturally to the value of ℓ = 0 (1, 2, 1, 2) for the mode with a period of 264.892 (261.444, 253.514, 215.291, 214.374) s given the a priori choice between ℓ = 0 or 1 (1 or 2, 1 or 2, 0 or 1, 1 or 2). These derived values are exactly the same as those used in the strong constraints experiment. Given the same values of ℓ, it follows that the optimization procedure also leads to the same values of k in order to match the same set of periods. Only the mode with a period of 201.430 s in our reference experiment is assigned a different ℓ (and k) identification compared to the strong constraints exercise as indicated by the boldface characters in the second group of two columns presented in Table 2. In that case, multicolor photometry allowed the possible partial identification ℓ = 0, 1, or 2 for that mode, and the optimization process operating during the weak constraints experiment led to the final identification ℓ = 0, k = 4, as compared to ℓ = 1, k = 5 in the strong constraints analysis. It should be pointed out, in this context, that the 201.430 s mode is the smallest amplitude mode for which useful partial mode discrimination could be carried out on the basis of the multicolor data set described by Charpinet et al. (2008).

The results of the no a priori ℓ identification experiment (the third group of two columns in Table 2) are even more interesting. We first point out that for six modes out of ten, the *derived* ℓ and k identifications are the *same* as those of the two previous experiments, thus insuring automatically, but after the fact, consistency with the constraints imposed by multicolor photometry. At the same time, the four modes identified by boldface characters are, on the contrary, in clear conflict with the results of multicolor photometry. In particular, the 356.194 s pulsation is the largest amplitude mode observed in BAL 0901, it is a singlet, and it has been formally identified as a radial mode. There can be no doubt as to its ℓ = 0 nature (see Charpinet et al. 2008). Likewise, the 354.008 s mode is the central component of a triplet that has also been formally identified as a dipole mode. And the 350.171 s pulsation is the central component of a multiplet formally identified through multicolor photometry as a quadrupole mode. Hence, at face value, the seismic model derived in this asteroseismological exercise should be rejected because it does not pass the test provided by independent multicolor photometric measurements. It is this model that we would have retained in the absence of external constraints provided by the multicolor data, as we did in all our previous analyses of other pulsating EC 14026 stars. Yet, Table 2 also reveals that this model is perfectly acceptable. It is, in fact, practically indistinguishable from our best formal seismic model, that is the one derived in the course of our reference experiment involving weak a priori constraints.

This state of affairs may seem somewhat surprising at first sight, but it finds a logical explanation in how p-mode pulsation spectra are organized in sdB stars. Indeed, p-modes of different ℓ indices but with the same values of k (k + 1 for dipole modes) tend to have comparable periods in sdB star models. For instance, the k = 0, ℓ = 0, 2 and k = 1, ℓ = 1 modes shown in Table 3 have periods of 353.89, 353.43, and 357.63 s, respectively. These 3 modes of differing ℓ-degrees therefore occupy a narrow interval which half-size, ∼2.1 s or ∼0.59% is comparable to the actual accuracy of the optimal model at the level of the period fit (see Table 3 and Sect. 3.3). Hence, even if the optimization procedure zooms in on a particular model mode with given ℓ and k, it is possible, even probable in several cases as our models are far from perfect, that the corresponding mode in the real star with a comparable period (e.g., the observed period at 356.194 s) has a different ℓ value (but the same k or k + 1 index). This situation has been encountered before and briefly commented on by Brassard & Fontaine (2008) in their study reporting on the first results obtained with their so-called third generation models. Briefly, Brassard & Fontaine (2008) reanalyzed a set of ten observed periods in the EC 14026 pulsator PG 0014+067 with the help of improved models. That star had been the subject of a first study by Brassard et al. (2001). Most interestingly, Brassard & Fontaine (2008) found essentially the same optimal seismic solution found earlier, but the mode identification (the ℓ indices) was only partially recovered. The bunching of the periods of modes with different ℓ indices and with the same values of k was proposed as an explanation, and we emphasize the same idea here.

The most interesting and significant result coming out of our numerical experiments is that the way we derive our seismic models is a very robust method that has proven to be quite insensitive to a priori partial mode identification. Hence, some misidentifications of the ℓ values of some modes can sometimes occur in our procedure, but this has hardly any practical consequences, at the presently achieved level of accuracy, on the

Table 3. Mode identification derived from asteroseismology and details of the fit. This corresponds to the optimal model derived using the weak constraints from multicolor photometry. The average properties of the fit are: $\overline{\Delta P/P} \simeq 0.59\%$, $\overline{\Delta P} \simeq 1.47$s, $\overline{\Delta\nu} \simeq 24.2\ \mu$Hz.

ℓ	k	$P_{\rm obs}$ (s)	$P_{\rm th}$ (s)	σ_I (rad/s)	log E (erg)	C_{kl}	$\Delta P/P$ (%)	ΔP (s)	Constraints
0	5	...	172.8235	$+1.415 \times 10^{-4}$ (S)	39.662	...	...	...	
0	4	201.4300	202.8432	$+2.164 \times 10^{-5}$ (S)	40.078	...	−0.7016	−1.4132	$\ell = 0, \underline{1}, 2$
0	3	...	223.2115	-3.735×10^{-6} (U)	40.473	...	...	...	
0	2	264.8920	265.8604	-2.179×10^{-5} (U)	40.460	...	−0.3656	−0.9684	$\ell = \underline{0}, 1$
0	1	...	301.2893	-1.008×10^{-6} (U)	41.847	...	...		
0	0	356.1940	353.8904	-3.742×10^{-6} (U)	41.226	...	+0.6467	+2.3036	$\ell = \underline{0}$
1	5	...	198.4887	$+2.468 \times 10^{-5}$ (S)	40.131	0.01438	...	...	
1	4	215.2910	217.9768	-8.867×10^{-7} (U)	40.279	0.01473	−1.2475	−2.6858	$\ell = 0, \underline{1}$
1	3	261.4440	263.8016	-2.121×10^{-5} (U)	40.459	0.01499	−0.9018	−2.3576	$\ell = \underline{1}, 2$
1	2	...	290.3820	-2.159×10^{-6} (U)	41.500	0.03321	...	...	
1	1	354.0080	353.4284	-3.767×10^{-6} (U)	41.220	0.01991	+0.1637	+0.5796	$\ell = \underline{1}$
2	5	...	189.1489	$+3.295 \times 10^{-5}$ (S)	40.161	0.03841	...	...	
2	4	214.3740	211.8767	$+7.486 \times 10^{-6}$ (S)	40.099	0.02231	+1.1649	+2.4973	$\ell = 1, \underline{2}$
2	3	253.5140	253.0446	-1.053×10^{-5} (U)	40.675	0.08081	+0.1851	+0.4694	$\ell = 1, \underline{2}$
2	2	...	272.3957	-1.381×10^{-5} (U)	40.664	0.05139	...	...	
2	1	350.1710	349.4887	-2.866×10^{-6} (U)	41.321	0.12218	+0.1948	+0.6823	$\ell = \underline{2}$
2	0	...	357.6339	-1.014×10^{-6} (U)	41.717	0.20566	...	...	
4	5	...	172.5637	$+1.359 \times 10^{-4}$ (S)	39.675	0.02963	...	...	
4	4	...	202.2717	$+2.414 \times 10^{-5}$ (S)	40.043	0.03480	...	...	
4	3	...	224.2660	-3.799×10^{-6} (U)	40.524	0.06699	...	...	
4	2	263.7360	264.5251	-2.110×10^{-5} (U)	40.451	0.02194	−0.2992	−0.7891	$\ell = \underline{4}$
4	1	...	313.1030	-7.663×10^{-7} (U)	41.940	0.13641	...	...	
4	0	...	350.8482	-3.550×10^{-6} (U)	41.211	0.02043	...	...	

derived structural parameters of a pulsator, the ultimate results that can come out of asteroseismology in our view. At first sight, this somewhat diminishes the impact and interest of using empirical identification techniques that provide information on the degree ℓ, from multicolor photometry, and possibly ℓ and m, from time-resolved spectroscopy, while radial orders k remain unspecified. We can also envision, however, that such misidentifications between modes having close periods will tend to disappear, as our long term efforts to improve the modeling of these stars by seeking more accurate fits of the observed periods progress. At that increased level of accuracy, we expect that constraints derived from independent mode identification techniques will play an important role in guiding our efforts toward the development of more physically accurate models for these stars.

3.3. Period fit and mode identification

In what follows, we retain the seismic model derived from our reference experiment, the one based on weak constraints and which is, therefore, fully compatible with the formal results obtained in the multicolor analysis of Charpinet et al. (2008). For this model, we find that the relative mean dispersion $\overline{\Delta P/P}$ between the ten observed and ten assigned model periods is equal to 0.59%. On an absolute scale, this corresponds to a mean value $\overline{\Delta P}$ of 1.47 s (or, equivalently, to a value $\overline{\Delta\nu}$ of 24.2 μHz). That sort of quality of the period fit is typical of that achieved in the asteroseismological analyses carried out so far on short-period sdB pulsators. Although quite good by general asteroseismological standards, the period match is far from perfect, and this reflects no doubt some inadequacies in our equilibrium models which could, admittedly, be improved. The work on "third generation" models reported by Brassard & Fontaine (2008), for instance, is a step in that direction.

Table 3 provides the specific assignment of each of the ten observed periods $P_{\rm obs}$ to ten theoretical values $P_{\rm th}$ belonging to the model period spectrum. Along with the degree ℓ and radial order k of the theoretical modes, the table also lists the stability coefficient σ_I, the logarithm of the kinetic energy log E, and the dimensionless first-order solid rotation coefficient C_{kl}. Note that the symbol (S) in the stability coefficient column stands for a stable (damped) pulsation mode, while (U) stands for an unstable (excited) one. The table also gives the relative and absolute differences in period for each pair $(P_{\rm obs}, P_{\rm th})$. Finally, the last column recalls the results of the multicolor photometry of Charpinet et al. (2008); the underlined value of ℓ indicates the best χ^2 solution (strong constraints).

As can be seen from the table, the ten periods that we retained in our analysis are identified with radial ($\ell = 0$) and non-radial ($\ell = 1 - 4$) p-modes of low radial order ($k = 0 - 4$). In this, BAL 0901 is no exception compared to what was found previously in other short-period sdB pulsators. All but two of the observed modes are predicted to be excited (negative values of σ_I in Table 3) by the κ-mechanism produced by the radiative levitation of iron according to our nonadiabatic calculations. The two exceptions, the 201.430 s and 214.374 s pulsations, fall just outside the predicted band of unstable periods for that model. They should not cause great concern because small imperfections in the model, which is very close to the red edge of the theoretical instability strip, could very well be at the origin of this effect. The two modes are indeed only marginally stable, with small positive values of σ_I compared to those of other stable modes. Alternatively, it may be that our estimate of the effective

temperature of BAL 0901 is slightly too low. For instance, an increase of $T_{\rm eff}$ by ~500 K is sufficient to excite the two recalcitrant modes in the hotter model.

We recall, in this context, the discussion of Charpinet et al. (2005b) concerning the existence of possible degenerate solutions within the framework of our approach, particularly a degenerate relationship in the S^2 hyperspace between the effective temperature and the total mass of sdB models. This is why an independent constraint on $T_{\rm eff}$ imposed by spectroscopy can be so useful, as such degeneracy between possible solutions can then be lifted. Given the uncertainties on the spectroscopic solution associated with the presence of metals in its atmosphere, it could very well be the case that the true temperature of BAL 0901 is closer to 28 500 K than the 28 000 K value that we used in our asteroseismological exercises. This would solve the "driving problem" discussed just above for the 201.430 s and 214.374 s modes. Beyond that, we explicitly checked, with the help of test calculations carried out with fixed effective temperatures in the relatively wide interval 28 000 ± 1200 K, how the inferred seismic solutions would behave. Quite interestingly here, we found that the total mass would increase by some 0.03 $M_\odot$ in going from $T_{\rm eff}$ = 26 800 K to $T_{\rm eff}$ = 29 200 K, a quite modest variation. At the same time, the other primary quantities (log g, and log q(H)) were found to be essentially unchanged.

Another point of interest related to the mode identification presented in Table 3 is about the distribution of the observed modes in relation to the model spectrum. As in several other cases analyzed in the past, we find that the observed period distribution in BAL 0901 appears to have "holes" in it. Indeed, one can legitimately raise the question of where are the 223.2 s ($\ell = 0$, $k = 3$), 301.2 s ($\ell = 0$, $k = 1$), 290.3 s ($\ell = 1$, $k = 2$), 272.3 s ($\ell = 2$, $k = 2$), and the other modes that are predicted to be unstable? We do not know the answer to that question. Again, we emphasize that this phenomenon has been observed in several other EC 14026 stars for which detailed asteroseismological analyses have been conducted. We can only speculate that either 1) the missing modes are excited in the real pulsator, but at amplitude levels below the detection threshold[3], or 2) some nonlinear effects determine how the available pulsational energy gets actually distributed among the many potentially excited modes.

We finally point out that there are many more modes detected in BAL 0901 than the ten $m = 0$ components that we used in this work. However, no useful constraints from multicolor photometry were obtained for these low-amplitude modes. A majority of these extra pulsations are nonlinear combinations of the ten dominant modes, but there are also several genuine modes with very long periods corresponding to mid-order g-modes. We are looking forward to exploit the asteroseismological information contained in these g-modes, as this will provide a welcome opportunity to refine further our seismic model of BAL 0901. This will have to wait the complete availability of improved models, however, as the current ones are not suitable for precise computations of the periods of g-modes (see, e.g., Randall et al. 2006a).

3.4. Structural parameters of BAL 0901

The three distinct asteroseismological exercises that we carried out led to almost identical sets of derived parameters, with no significant differences between them. In the following, however, we specifically adopt the formal seismic solution obtained in our reference experiment. This optimal model, identified in Sect. 3.2, leads to the determination of the fundamental parameters that define the structure of BAL 0901 as summarized in Table 4. The three primary quantities that are naturally derived from the asteroseismic procedure are the surface gravity log g, the hydrogen-rich envelope mass log($M_{\rm env}/M_*$), and the stellar mass M_*, whereas the fourth one, the effective temperature $T_{\rm eff}$, is obtained from spectroscopy (see discussion above). A set of secondary parameters then follows from the values obtained for the primary quantities: the stellar radius R (as a function of M_* and g), the luminosity L (as a function of $T_{\rm eff}$ and R), the absolute magnitude M_V (as a function of g, $T_{\rm eff}$, and M_* in conjunction with the use of a detailed model atmosphere), and the distance from Earth d (as a function of V and M_V). Estimates of the 1σ (internal) errors associated with the primary quantities are calculated following the recipe described in detail by Brassard et al. (2001) and Charpinet et al. (2005a). These errors are represented in Fig. 2 by white dashed contours (1, 2, and 3σ limits) around the solution indicated by the yellow mark. The rotation period of BAL 0901 can also be determined from the interpretation of the regular frequency spacings present in its pulsation spectrum (the multiplet structures briefly referred to above), assumed to be caused by rotational splitting. Treated as a first-order perturbation (which is fully justified in the case of a slow rotator like BAL 0901), and assuming solid body behavior, rotation leads to a period given by,

$$P_{\rm rot} = \frac{1 - C_{kl}}{\Delta\nu_{kl}} \qquad (2)$$

where $\Delta\nu_{kl}$ is the frequency spacing (Hz), $P_{\rm rot}$ is the rotation period (s), and C_{kl} is the dimensionless first-order rotation coefficient (see Table 3). Baran et al. (2005), from observations gathered over a one month timebase, determined a mean frequency spacing of about $\overline{\Delta\nu}$ = 1.58 μHz with a standard deviation of $\sigma(\Delta\nu) \simeq 0.12$ μHz. In comparison, the multisite campaign of August 2005 reported on by Pereira et al. (2008) was more limited in frequency resolution and spacings less than ~2 μHz could not be established with accuracy, although there were obvious numerous close frequencies, preferentially distributed at even multiples of $\overline{\Delta\nu}$. For our present needs, we thus adopted the results of Baran et al. (2005). On the theory side, we can compute an average value of the quantity $\overline{D} \equiv \overline{1 - C_{kl}} = 0.958 \pm 0.042$. Using these average values in Equation (2), a rotation period of $P_{\rm rot}$ = 7.02 ± 0.85 days is derived. Finally, the rotation period combined with the asteroseismic estimate of the star radius leads to the determination of the equatorial rotation velocity $V_{\rm eq} = 2\pi R/P_{\rm rot} = 1.59 \pm 0.23$ km s^{-1}. To our knowledge, there

Table 4. Inferred properties of BAL 0901 (V = 12.1 ± 0.1).

Quantity	Estimated value
$T_{\rm eff}$ (K)	28000 ± 1200
log g	5.383 ± 0.004
$M_*/M_\odot$	0.432 ± 0.015
log($M_{\rm env}/M_*$)	−4.89 ± 0.14
$R/R_\odot$ (M_*, g)	0.221 ± 0.005
$L/L_\odot$ ($T_{\rm eff}$, R)	27.2 ± 6.5
M_V (g, $T_{\rm eff}$, M_*)	4.02 ± 0.14
d (V, M_V) (pc)	412 ± 45
$P_{\rm rot}$ (d)	7.02 ± 0.85
$V_{\rm eq}$ ($P_{\rm rot}$, R) (km s^{-1})	1.59 ± 0.23

[3] For instance, the multisite campaign reported by Pereira et al. (2008) has revealed, among others, a low amplitude pulsation with a period of 276.102 s [their f_{25} mode] which, perhaps, could be associated with the 272.3 s theoretical mode with $\ell = 2$ and $k = 2$ in Table 3.

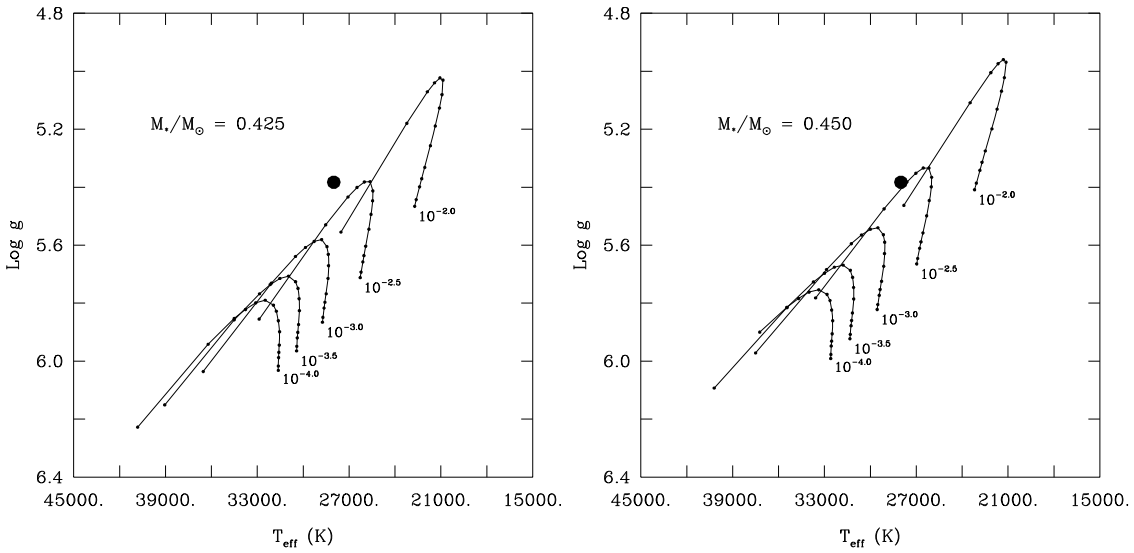

Fig. 3. *Left panel:* location of BAL 0901 (large dot) in the log $g - T_{\rm eff}$ diagram in comparison to the predictions of families of core helium-burning models with the same total mass $M_*/M_\odot = 0.425$, but with different values of the outer hydrogen layer mass $\log(M_{\rm env}/M_*)$ from −2.0 to −4.0. *Right panel:* similar, but for families of models with a total mass of $M_*/M_\odot = 0.450$.

exists as yet no accurate spectroscopic measurement of $V_{\rm eq}\sin i$ that could be used to infer or constrain the inclination of the pulsation/rotation axis of BAL 0901 with respect to the line of sight.

The structural parameters obtained for BAL 0901 are of special interest concerning the total mass and the hydrogen-rich envelope mass, two quantities that can not be derived using other means in this apparently single star. The total mass inferred lies somewhat below the canonical model value of ∼0.47 $M_\odot$, but still well within the various mass distributions expected for sdB stars, either from single star evolution (D'Cruz et al. 1996) or from several scenarios of binary evolution (Han et al. 2002, 2003). We recall here that our search domain for the total mass covered a very wide range of values for sdB stars, from 0.3 to $0.7 M_\odot$, following the recommendation of these last authors. We also point out that BAL 0901 does not show any clear evidence of a possible companion: the measured radial velocity variations in the spectra are completely dominated by the main pulsation mode according to Telting & Østensen (2006), and there is no spectroscopic signature of a cooler companion in the optical spectrum. In addition, the data from the 2MASS project reveal a $J-H$ index in the range from −0.103 to −0.163, and a $J-K$ index in the range from −0.159 to −0.229. Our detailed model atmosphere for BAL 0901 used in the determination of M_V above reveals, for its part, theoretical color indices of $J-H = -0.111$ and $J - K = -0.210$. Those are perfectly consistent with, and reinforce, the idea of a single star. Of course, if BAL 0901 had a faint white dwarf companion, its optical spectrum and infrared color indices would not be affected by its presence, but one would expect such a system to form a close binary with a relatively short orbital period that would leave a strong radial velocity signature, which has not been observed.

A most interesting result emerges from our seismic solution concerning the evolutionary status of BAL 0901. From its location in the log $g - T_{\rm eff}$ diagram as obtained by spectroscopy, there is already a hint that BAL 0901 is likely to be in a phase beyond the Terminal Age Extreme Horizontal Branch (TAEHB): its surface gravity being relatively small for a typical sdB with $T_{\rm eff} = 28\,000$ K. This suggestion is very strongly reinforced in the light of our seismic solution which reveals that the combination of the four primary parameters derived in our analysis is incompatible with the idea that BAL 0901 is currently burning helium in its center. This is best demonstrated with the help of Fig. 3, which compares the actual location of BAL 0901 in the log $g - T_{\rm eff}$ plane with those of families of *core helium-burning models* with different assumed hydrogen-rich envelope masses. We picked the values of the total mass $M_*/M_\odot = 0.425$ and 0.450 (left and right panel of Figure TAEHB, respectively) in order to sandwich our asteroseismologically determined value of $M_*/M_\odot = 0.432$. The models illustrated belong to the so-called third generation (see Brassard & Fontaine 2008) and cover only the core helium-burning phase, from the ZAEHB to near the TAEHB. These models incorporate a variable and nonuniform iron abundance profile as obtained from the assumption of diffusive equilibrium between radiative levitation and gravitational settling. From the results shown in Fig. 3, it is easily seen that our argument in favor of the idea that BAL 0901 is in a post-TAEHB phase strongly hinges on the fact that our derived value of the hydrogen layer mass, $\log(M_{\rm env}/M_*) = -4.89$, is unusually small. If this estimate is correct, then there is no way to account for BAL 0901 as a core helium-burning object, as can be obviously inferred from the figure.

An additional independent argument further reinforces this conclusion. As part of the ongoing effort to adapt our forward modeling approach to the third generation equilibrium structures, huge grids of stellar models are being computed, and several millions of them are already available. As briefly alluded to above, it should be emphasized that these models currently cover *only* the core helium-burning phase of the evolution of sdB stars; they do not extend to the shell-burning phase and beyond. Using the adiabatic approximation (which is amply sufficient to compute accurate periods in the present context), we pulsated all of the numerous available third generation models in search of the one that would provide the best period match to the set of ten periods observed in BAL 0901 as used in this paper. Of course, only models compatible with the spectroscopic constraints on $\log g$ and $T_{\rm eff}$ were eventually retained, and we used the no a priori approach with respect to mode identification, thus allowing the observed modes to belong to ℓ index values of 0, 1, 2,

or 4. Contrary to the case of the pulsating EC 14026 star PG 0014+067 for example (and see Brassard & Fontaine 2008), we could not find a single model that would provide a satisfactory fit to the observed periods. In the best case, the merit function S^2 ended up a huge factor of five larger than the value $S^2 \simeq 0.249$ derived previously in our reference study above. We conclude from this, and this conclusion is very strong in our view, that BAL 0901 cannot be currently burning helium in its center. It is then most likely in a post-TAEHB phase.

The set of model parameters that best explains the observed period structure of BAL 0901 remains that given in Table 4, including the low value of the hydrogen envelope mass. How to "make" a sdB star with such a thin envelope given the values of its effective temperature, surface gravity, and total mass, is a question whose answer currently eludes us. At this stage, we can only speculate and hope that our results might stimulate other researchers. We point out, for instance, that Feige 48 at $\log g = 5.46$ and $T_{\rm eff} = 29\,580$ K, is not very far from BAL 0901 in the $\log g - T_{\rm eff}$ diagram, near the common boundary between the EC 14026 domain and the domain where long-period pulsators are found (see, e.g., Fig. 2 of Fontaine et al. 2006). However, the asteroseismic analysis of Van Grootel et al. (2008) has revealed that the hydrogen layer mass in Feige 48 is "normal" at a value of $\log(M_{\rm env}/M_*) = -2.52$ which, combined to its values of $\log g$, $T_{\rm eff}$, and M_*, suggests a core helium-burning object. So, could it be that the change of phase, from post-ZAEHB object in the case of Feige 48 to post-TAEHB star for BAL 0901 has something to do with the fact that the latter pulsates in both short- and long-period modes, while the former shows only short-period pulsations? Clearly, detailed asteroseismological studies of the two other known hybrid pulsators, HS 0702+6043 and HS 2201+2610, become particularly justified in this context.

We may also speculate about the effects of a stellar wind on the structure of sdB stars. According to Fontaine & Chayer (1997) (and see also Unglaub & Bues 2001), a wind of order 10^{-14}–10^{-13} $M_\odot$ yr^{-1} is necessary to maintain the helium abundances at their observed levels in the atmospheres of sdB stars. Otherwise, without the competing effect of the wind against gravitational settling, only very small traces of helium, much smaller in fact than those generally observed, could remain in such atmospheres via radiative levitation. If BAL 0901 is really a post-TAEHB as we propose, it must have lived at least 10^8 yr as a sdB star in the post-ZAEHB phase. Assuming that a typical wind of 10^{-14}–10^{-13} $M_\odot$ yr^{-1} has operated on the average during this relatively long period in the life of BAL 0901, then only a mass fraction of $\log \Delta M/M_* \simeq -5.6$ to -4.6 could have been lost in the post-ZAEHB phase, much too small to have thinned down significantly a hydrogen layer containing, say, $\log(M_{\rm env}/M_*) \simeq -2.5$. So, could it be instead that mass loss becomes much more important immediately following core helium exhaustion, when instabilities associated with shell helium burning set in? In this way, one could envision a post-TAEHB phase during which the outer hydrogen layer rapidly thins down. We suggest that, perhaps, this has been the recent fate of BAL 0901.

4. Summary and conclusion

This paper reported on a detailed asteroseismological analysis of BAL 0901, the brightest of the known pulsating sdB stars, and one that exhibits large amplitudes for its dominant modes. Because of these, BAL 0901 has been extensively studied over the last few years, including a very successful run carried out at the Canada-France-Hawaii Telescope to pin down or constrain the ℓ index of several pulsation modes through multicolor (UBV) photometry (see Charpinet et al. 2008). That study led to the partial identification of some ten independent pulsation modes, a number comparable to those used in previous asteroseismic analyses of other pulsating sdB stars. We took advantage of the availability of these results to test our approach to the asteroseismology of sdB stars through the forward method. This is based on a double optimization search technique that aims at finding the optimal model in parameter space, i.e., the one that best matches the observed periods with a set of computed periods. In our previous efforts, in the absence of constraints on the values of ℓ for the observed modes, the search was carried out with no a priori assumptions as to the degree indices of the modes, except for some general considerations based on visibility arguments. In those cases, mode identification comes out naturally as a *byproduct* of the global fitting procedure. The independent constraints on the ℓ values obtained from the multicolor analysis of Charpinet et al. (2008) opened up, for the first time in the sdB field, the possibility of testing our asteroseismic method at the level of mode identification, but also, and even more importantly from our point of view, at the level of the reliability and robustness of the stellar parameters that we derive in the process. In order to do that, we have repeated the optimization procedure three times, using various assumptions as to the values of the ℓ indices of the ten retained modes in BAL 0901. Our reference experiment is based on what we called weak constraints on the ℓ values, i.e., those corresponding to all the formally acceptable values that came out of the Charpinet et al. (2008) study. A second experiment used strong constraints, i.e., we assigned a priori a single value of ℓ (the one giving the smallest χ^2 in those cases with multiply acceptable choices) to each of the ten modes under consideration. And finally, in a third experiment, we used no a priori constraints to mimic what has been done in all our previous asteroseismological analyses of pulsating sdB stars.

The results presented in this paper demonstrate beyond any doubt that the approach we have developed for the asteroseismology of sdB stars is sound and reliable. Indeed, the tests carried out are quite conclusive. Our most significant finding is that the asteroseismological solution (the optimal model) stands very robust, whether or not external constraints on the values of the degree ℓ are used. Even though some modes may have been misidentified in ℓ in the no a priori experiment, the optimal models that came out of the calculations turned out to be practically the same in all three exercises. This result, which may seem somewhat surprising at first sight, finds a natural explanation in the very structure of the p-mode pulsation spectra of sdB stars. In particular, modes with the same values of k, but different ℓ's, tend to bunch together in period, while they exhibit larger period spacings if they have different radial order indices k. Hence, it is easy to imagine that small inadequacies in models may lead the search algorithm – designed to minimize the merit function S^2 – to pick a theoretical mode with, say, ℓ and k, while the real mode has a very similar period and the same value of k, but another value of the degree index, for example ℓ'. In that instance, the ℓ identification would come out wrong, but the periods of the two modes are so similar that the merit function S^2 would not have been seriously degraded had the algorithm picked the correct mode (with a period slightly worse than the one picked in comparison with the observed period). It therefore follows that the procedure leads to the same optimal model in practice, irrespective of possible small shortcomings in the models. This finding is far-reaching and can be applied retroactively to our previous analyses of pulsating sdB stars. In particular, the after-the-fact mode identifications that came out of these studies might

be wrong in some cases (in the ℓ identification, not in k), but the stellar parameters inferred for the various pulsators that were studied should be quite reliable. We conclude from this, that a priori partial mode identification (through multicolor photometry and/or time-series spectroscopy) does not necessarily constitute an indispensable ingredient, at least for the determination of the structural parameters of pulsating sdB stars at the level of accuracy that is currently achieved. These techniques shall not be abandonned, however, since they will still provide precious guidelines when the accuracy of the asteroseismic fits will improve, as we progress in this long term quest dedicated at clarifying further the physical description of sdB models.

A very important byproduct of our study has been the determination of the basic structural properties of Bal 0901 as summarized in our Table 4. These estimates represent the ultimate product of our approach which combines spectroscopy and asteroseismology. They are of very high intrinsic interest. We find, in particular, that BAL 0901 is unusual in that we uncovered strong evidence that it cannot currently be burning helium in its center and, therefore, is most likely a star in a very advanced phase of evolution, a post-TAEHB object. We cannot explain satisfactorily at this stage why BAL 0901 has apparently a rather thin outer hydrogen envelope. We offered a speculation involving a stellar wind, but we hope that other researchers can follow up on this or come up with other viable possibilities. We also wish to point out that BAL 0901 is now the 8th pulsating sdB star for which a detailed asteroseismological analysis has been successfully carried out. Although this is a slow process, the present work constitutes one more step in our quest to determine the empirical mass distribution of sdB stars through this technique. Finally, in concluding this discussion, we want to emphasize the fact that the asteroseismological story of BAL 0901 is far from being completely told. And indeed, it will be very interesting in the future to tap the information contained in the long-period g-modes that are also observed along with the short-period oscillations that we exploited in this paper. This will require the full availability of our third generation stellar models, further improved to also deal with the highly evolved post-TAEHB H/He shell burning phase.

Acknowledgements. This work was supported in part by the NSERC of Canada. G.F. also acknowledges the contribution of the Canada Research Chair Program. This work made extensive use of the computing facilities offered by the Calcul en Midi-Pyrénées (CALMIP) project and by the Centre Informatique National de l'Enseignement Supérieur (CINES), France. Experiments presented in this paper were also carried out using the Grid'5000 experimental testbed, an initiative from the French Ministry of Research through the ACI GRID incentive action, INRIA, CNRS and RENATER and other contributing partners (see `https://www.grid5000.fr`).

References

Baran, A., Pigulski, A., Kozieł, D., et al. 2005, MNRAS, 360, 737
Baran, A., Oreiro, R., Pigulski, A., et al. 2006, Baltic Astron., 15, 227
Baran, A., Pigulski, A., & O'Toole, S. J. 2008, MNRAS, 385, 255
Bixler, J. V., Bowyer, S., & Laget, M. 1991, A&A, 250, 370
Blanchette, J.-P., Chayer, P., Wesemael, F., et al. 2008, ApJ, in press
Brassard, P., & Fontaine, G. 2008, in Proc. Third Meeting on Hot Subdwarf Stars and related Objects, ASPC, ed. U. Heber, R. Napiwotzki, & C. S. Jeffery, in press
Brassard, P., Pelletier, C., Fontaine, G., & Wesemael, F. 1992, ApJS, 80, 725
Brassard, P., Fontaine, G., Billères, M., et al. 2001, ApJ, 563, 1013
Brown, T. M., Ferguson, H. C., Davidsen, A. F., & Dorman, B. 1997, ApJ, 482, 685
Charpinet, S., Fontaine, G., Brassard, P., & Dorman B. 1996, ApJ, 471, L103
Charpinet, S., Fontaine, G., Brassard, P., et al. 1997, ApJ, 483, L123
Charpinet, S., Fontaine, G., & Brassard, P. 2001, PASP, 113, 775
Charpinet, S., Fontaine, G., & Brassard, P. 2003, in White Dwarfs, NATO ASIB Proc., 105, 69
Charpinet, S., Fontaine, G., Brassard, P., Green, E. M., & Chayer, P. 2005a, A&A, 437, 575
Charpinet, S., Fontaine, G., Brassard, P., et al. 2005b, A&A, 443, 251
Charpinet, S., Silvotti, R., Bonnano, A., et al. 2006, A&A, 459, 565
Charpinet, S., Fontaine, G., Brassard, P., et al. 2008, in Proc. Third Meeting on Hot Subdwarf Stars and related Objects, ASPC, ed. U. Heber, R. Napiwotzki, & C. S. Jeffery, in press
D'Cruz, N., Dorman, B., Rood, R. T., & O'Connell, R. W. 1996, ApJ, 466, 359
Dorman, B., Rood, R. T., & O'Connell, R. W. 1993, ApJ, 419, 596
Edelmann, H. 2003, Ph.D. thesis, Universität Erlangen-Nürnberg
Fontaine, G., & Brassard, P. 1994, in Stellar and Circumstellar Astrophysics, a 70th birthday celebration for K.-H. Böhm, & E. Böhm-Vitense, ASP Conf. Ser., 57, 195
Fontaine, G., &, Chayer, P. 1997, in Third Conf. on Faint Blue Stars, ed. A. Philip, J. Liebert, & R. Saffer, Schenectady: Davis, 169
Fontaine, G. Brassard, P., Charpinet, S., et al. 2003, ApJ, 597, 518
Fontaine, G. Brassard, P., Charpinet, S., et al. 2006, in ESA SP-624
Green, E. M., Fontaine, G., Reed, M. D., et al. 2003, ApJ, 583, L31
Han, Z., Podsiadlowski, P., Maxted, P. F. L., Marsh, T. R., & Ivanova, N. 2002, MNRAS, 336, 449
Han, Z., Podsiadlowski, P., Maxted, P. F. L., & Marsh, T. R. 2003, MNRAS, 341, 669
Heber, U. 1986, A&A, 155, 33
Heber, U., Reid, I. N., & Werner, K. 2000, A&A, 363, 198
Jeffery, C. S., & Saio, H. 2006, MNRAS, 372, L48
Jeffery, C. S., & Saio, H. 2007, MNRAS, 378, 379
Kilkenny, D., Koen, C., O'Donoghue, D., & Stobie, R. S. 1997, MNRAS, 285, 640
Koen, C., O'Donoghue, D., Pollaco, D. L., & Nitta, A. 1998, MNRAS, 300, 1105
Lutz, R., Schuh, S., Silvotti, R., et al. 2008, in Proc. Third Meeting on Hot Subdwarf Stars and related Objects, ASPC, ed. U. Heber, R. Napiwotzki, & C. S. Jeffery, in press
Oreiro, R., Ulla, A., Pérez Hernández, F., et al. 2004, A&A, 418, 243
Oreiro, R., Pérez Hernández, F., Ulla, A., et al. 2005, A&A, 438, 257
Østensen, R., Telting, J., & Heber, U. 2007, CoAst, 150, 265
Pereira, C., Jeffery, C. S., Fontaine, G., et al. 2008, MNRAS, in prep.
Randall, S. K., Fontaine, G., Brassard, P., & Bergeron, P. 2005, ApJS, 161, 456
Randall, S. K., Green, E.M., Fontaine, G., et al. 2006a, ApJ, 645, 1464
Randall, S. K., Fontaine, G., Charpinet, S., et al. 2006b, ApJ, 648, 637
Randall, S. K., Green, E. M., Van Grootel, V., et al. 2007, A&A, 476, 1317
Saffer, R. A., Green, E. M., & Browers, T. 2001, in 12th European Workshop on White Dwarfs, ed. J. L. Provencal, H. L. Shipman, J. MacDonald, & S. Goodchild, Astron. Soc. Pacific Conf. Ser., 226, 408
Schuh, S., Huber, J., & Dreizler 2006, A&A, 445, L31
Telting, J. H., & Østensen, R. 2006, A&A, 450, 1149
Tremblay, P. E., Fontaine, G., Brassard, P., et al. 2006, ApJS, 165, 551
Ulla, A., & Thejll, P. 1998, A&AS, 132, 1
Unglaub, K., & Bues, I. 2001, A&A, 374, 570
Van Grootel, V., Charpinet, S., Fontaine, G., & Brassard, P. 2008, A&A, 483, 875